Chapter 4
Conclusions and Discussions

Through this work, a model of disordered structure of porous silicon is proposed. An irregular structure of porous silicon is assumably produced by removals of some silicon atoms randomly from a perfect crystalline silicon and all dangling bonds are terminated by hydrogen atoms. We also assume that there is no reconstruction around vacancies. Removals of some atoms are represented by the occurring of potential barriers, which equivalents to the generating of potential wells among the barriers. Then porous silicon can be modelled as a disordered assembly of three-dimensional quantum wells which are produced from random potential fluctuation from the system. All quantum wells are assumed to have Gaussian form for simplicity. The model directly leads to the reduction of density of states near the band edges of crystalline silicon (Figure 2.1 and 3.1) which seems to be band-gap widening as found in the quantum confinement model (crystalline silicon model). Actually, our model is classified to be a quantum confinement model category. The localization of carriers and the upshift of states near bulk crystalline band edge are, indeed, due to size effect. Our model is just a modified model formed by addition of disorder into the ordinary crystalline silicon model then it is not surprised that many results are in the same way as that of original crystalline silicon model.

There are two important advantages of our model over others' when porous silicon is treated as a disordered system. First, it allows us to do the investigation using Feynman's path-integral of disordered system (Samathiyakanit, 1974; Sa-yakanit, 1979). So the analytical approximated density of states closed

to the band edge is obtained (eq.(2.81)) :

$$\begin{aligned}\rho(E) &= \frac{1}{2\pi\hbar}\int_{-\infty}^{\infty} dt \left(\frac{m}{2\pi i\hbar t}\right)^{3/2}\left(\frac{\gamma t}{\sin(\gamma t/2)}\right)^{3} \\ &\quad \cdot \exp\left[\frac{i}{\hbar}(E-E_0)\,t + \frac{3}{2}\left(\frac{1}{2}\gamma t\cot\gamma\frac{t}{2}-1\right)\right. \\ &\quad \left. -\frac{\xi_L}{2\hbar^2}\left(\frac{L^2}{4}\right)^{3/2} t\int_0^t dy\left(B(y)+\frac{L^2}{4}\right)^{-3/2}\right],\end{aligned} \tag{4.1}$$

as well as its low-energy limit (eq.(2.89)),

$$\rho_L(\eta;z) = \frac{L^{-3}}{E_L\xi_L'^{5/4}}\frac{a(\eta;z)}{b^{3/4}(\eta;z)}\exp\left[\frac{-b(\eta;z)}{4\xi_L'}\right] D_{3/2}\left(\sqrt{\frac{b(\eta;z)}{\xi_L'}}\right), \tag{4.2}$$

and high-energy limit (eq.(2.97)),

$$\rho(\eta) = \frac{m^{3/2}}{\pi^2\hbar^3}\xi_L^{1/4}\exp\left[-\frac{\eta^2}{4\xi_L}\right] D_{-3/2}\left(\frac{\eta}{\sqrt{\xi_L}}\right). \tag{4.3}$$

The low- and high-energy limit density of states of porous silicon are shown graphically in Figures 2.2 and 2.1 respectively. Then, the band-gap widening can clearly be observed from the obtained density of states. Furthermore, treating a porous silicon as a disordered system also implies the existence of mobility gap which is important part to explain electrical conduction mechanism of porous silicon which consists of hopping via localized states and extended states conduction (Lubianiker and Balberg, 1997) as discussed previously in Section 1.4.4. Such mechanisms cannot be explained in the ordinary crystalline silicon model. In addition, in our model, the mobility gap of porous silicon, E_g', is roughly estimated as a function of porosity, p, as well (eq.(2.110)) :

$$E_g' = E_g + 2v_0n_0\left(\frac{p}{100}\right)\left(\frac{\pi a_0^2}{4\ln 2}\right)^{3/2}. \tag{4.4}$$

It is important to point out that our model can imply both optical and electrical properties of the porous silicon. In addition, the expression (4.1) is the

first analytical expression of density of states of porous silicon which is obtained from our more realistic structure of porous silicon. Moreover, our proposed model can be generally applied to other porous semiconductors which originated from crystalline semiconductors (Sukpitak, Sa-yakanit and Sritrakool, 2003).

However, our model has still been incomplete. The scatterer strength v_0 cannot be directly obtained from the model. By using the advantage of our model that can relate to electrical properties of porous silicon, the scatterer strength can then be related to the activation energy of extended state conduction E_a as expressed in eq.(2.114)

$$v_0 \cong \left(E_a - \frac{E_g}{2}\right)\left(\frac{100}{pn_0}\right)\left(\frac{\pi a_0^2}{4\ln 2}\right)^{-3/2}. \tag{4.5}$$

Using eq.(4.5) or (2.114) together with experimental data of activation energy (Lee et al., 1996), we can obtained the scatterer strengths at various levels of porosity and can be used in the numerical calculations (Table 2.2 and Figure 2.3).

In order to verify our model, a numerical calculation from our model is needed to compare with experiments. The calculation of optical absorption coefficient is the most suitable one since it can be related directly to the density of states. The calculation is comfortable and gives more reliable result if dealing with direct-gap porous semiconductors such as GaAs or InP at first, in order to avoid phonon-assisted transitions. Unfortunately, most studies reported to date concern porous silicon and a few indirect gap semiconductors. There are a few reports on GaAs (Beale et al., 1985; Schmuki, Lockwood, Labé et al., 1996) and on InP (Takizawa, Arai and Nakahara, 1994; Kikuno, Amiotti, Takizawa et al., 1995) but there is no experimental absorption results that we need.

In case of optical absorption of porous silicon, there are a number of evidence which indicate that the transitions are phonon-assisted (Kovalev et al., 1996; Datta and Narasimhan, 1999). This means that non-phonon assisted processes are small or no contribution to the optical absorption, contrast to the photoluminescence of porous silicon which involves with both non-phonon and phonon assisted processes (Hybertsen, 1994; Kovalev et al., 1998).

In order to examine this contradiction, we calculate the optical absorption coefficients using the obtained density of states (eq.(3.39)) together with a simple model of optical absorption as discussed in Chapter 3. However, because of the unclear band structure of porous silicon, it is impossible to calculate the absorption coefficients which take care rigorously both non-phonon and phonon assisted processes. Here, we focus ourselve on non-phonon assisted processes which can occur only when it involves with localized states because wave functions of localized states widely spread in momentum space then the non-phonon assisted process can occur. On the other hand, such a process cannot occur in transitions between delocalized states with well-defined wave vectors. Thus, we neglect all between delocalized states in our calculation. We also assume that all transitions of interest are direct-gap transitions, as a result, although the calculated absorption coefficients are overestimated in magnitude but still be enough to determine the energy range of the non-phonon assisted process.

The calculation results are shown in Figures 3.1-3.8. For porous silicon with over 70% porosity, the calculated absorption coefficient shown by a peak appears. The height of this peak is comparable to the value of the experimental results, within the narrow particular energy range. On the other hand, for porous silicon with less than 65% porosity, the calculated results are about 0 cm^{-1} which

indicate that non-phonon assisted transition can be completely ignored. However, because of overestimation of the assumption, this can imply that non-phonon assisted transition can be neglected in an optical absorption process as suggested by many authors (Kovalev et al., 1996; Datta and Narasimhan, 1999).

Furthermore, the expected absorption closed to the band gap of bulk crystalline silicon is not found for all cases in our calculations since there are no states near bulk crystalline silicon band edge in our model. However, this contrasts with the experimental results such as that of Xie et al. (1994) and Datta and Narasimhan (1999), which have significant absorption near bulk crystalline band gap. This means that there are a large number of states in porous silicon, near band edges of bulk crystalline. Such states require an existence of a large nanocrystal size in porous silicon but it does not exist in our model since our porous structure model is obtained by removals of some silicon atoms randomly. Then the remaining of nanocrystal would have a size distribution form of Gaussian with small variance. So, in order to explain all spectrum of optical absorption, it is essential to seriously involve the nanocrystal's size distribution in the calculation. The important role of size distribution is emphasized recently in work of Datta and Narasimhan (1999) which suggests the distribution $P(d)$ of lognormal form,

$$P(d) \propto \frac{1}{\ln(\sigma_L)\, d} \exp\left[-\frac{(\ln(d) - \ln(d_0))^2}{2(\ln(\sigma_L))^2}\right] \tag{4.6}$$

where d_0, σ are mean size and its standard deviation respectively. A lognormal and Gaussian distribution are shown in Figure 4.1. In addition, we also suggest for future work that the size distribution can include to our model by considering porous silicon consisting of subsystems of various porosity.

Consequently, from our model, we calculate scatterer strength from the experimental results of activation energy (Lee et al., 1996) as shown in Figure

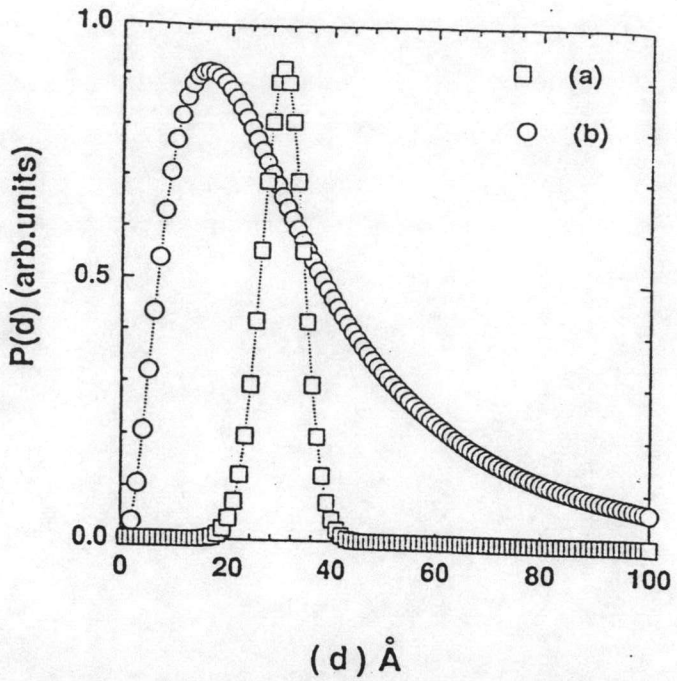

Figure 4.1: Size distribution (a) for a Gaussian and (b) for a lognormal distribution of widths, having $d_0 = 30$ Å and $\sigma = 4$ Å (Datta and Narasimhan, 1999)

2.3 and Table 2.2. We found that the calculated scatterer strength seems to be an increasing function of porosity which contrasts with our assumption. In our model, the scatterer strength is assumed to be a constant at all porosity contents. However, it is obviously seen that existence of perfect potential wells essentially require occurrence of a large number of scatterers (high porosity). At low porosity, the wells do not have perfect shape as in the model. The well shape is broader and lower in height than that of our model. Then we believe that porosity dependent behavior of scatterer strength can indicate the perfection of potential wells in our model. In addition, there is a significant stable of scatterer strength at 70-80% porosity. This can imply that our model potential wells become perfect shape at around 70% porosity.

Moreover, it is interesting to consider the associated confinement energy in each case, as shown in Table 4.1. We found that all cases, which non-phonon assisted transition significantly involved, have confinement energy of about 0.8

Porosity (%)	Confinement energy (eV)		
	T = 7K	T = 100K	T = 300K
80	0.85	0.85	0.85
71	0.80	0.79	0.79
65	0.29	0.29	0.29
60	0.03	0.03	0.03

Table 4.1: Calculated confinement energy for all cases of study

eV. While all cases, which are not participated by non-phonon assisted transition, have confinement energy below 0.3 eV. This coincides with the work of Kovalev et al. (1998) in study of a ratio between the non-phonon assisted process and the phonon-assisted process in luminescence of silicon nanocrystal. They suggest that non-phonon transitions begin to dominate at confinement energy about 0.7 eV.

Finally, at here, the validity of our model is discussed. According to our model, the random potential wells are generated from occurrence of random scatterers. It is obviously seen that the existence of the potential wells needs occurrence of a large number of scatterers. This implies that our model is not valid in low porosity region. In addition, the investigation of relation between scatterer strength and porosity (Figure 2.3) indicates that scatterer strength has a reasonable when porosity exceed 60%. Therefore, the lower limit of porosity applied to our model is reasonably about 60%.